PAX2 induces vascular-like structures in normal ovarian cells and ovarian cancer

KHOLOUD ALWOSAIBAI[1-3], ENSAF M. AL-HUJAILY[2-4], SALMAH ALAMRI[1], SALIM GHANDORAH[5], KENNETH GARSON[2,3] and BARBARA C. VANDERHYDEN[2,3]

[1]Biomedical Research Department, Research Center, King Fahad Specialist Hospital, Dammam 32253, Saudi Arabia; [2]Department of Cellular and Molecular Medicine, University of Ottawa, Ottawa, ON K1N 6N5; [3]Cancer Therapeutics Program, Ottawa Hospital Research Institute, Ottawa, ON K1Y 4E9, Canada; [4]Cell Therapy and Cancer Research Department, King Abdullah International Medical Research Center, King Abdulaziz Medical City, Ministry of National Guard Health Affairs, Riyadh 11426; [5]Department of Pathology and Laboratory Medicine, King Fahad Specialist Hospital, Dammam 32253, Saudi Arabia

Received September 6, 2021; Accepted March 9, 2022

DOI: 10.3892/etm.2022.11339

Abstract. In adult tissue, the paired box 2 (PAX2) protein is expressed in healthy oviductal, but not normal ovarian surface epithelial cells. PAX2 is expressed in a subset of cases of serous ovarian carcinoma; however, the role of PAX2 in the initiation and progression of ovarian cancer remains unknown. The aim of the present study was to determine the biological effects of PAX2 expression in normal and cancerous epithelial cells. By culturing the normal and cancerous ovarian cells that express PAX2 in 3D culture and staining the cells with vasculogenic mimicry markers such as CD31 and PAS, it was shown that PAX2 overexpression in both normal and cancerous ovarian epithelial cells induced formation of vascular-like structures both *in vitro* and *in vivo*. These results indicated a potential role of PAX2 in ovarian cancer progression by increasing the presence of vascular-like structures to promote the supply of nutrients to tumor cells and facilitate cancer cell proliferation and invasion.

Introduction

Ovarian carcinomas are heterogeneous with few identified causative genetic mutations (1); they also exhibit genomic aberrations associated with altered gene expression that also has been reported in breast cancer (2). Paired box 2 (PAX2) protein expression is upregulated in certain types of ovarian cancer, including endometrioid ovarian cancer, as well as clear cell, mucinous and serous carcinoma (3). However, its role in promoting tumor progression is not yet clear. PAX2 serves important roles in embryogenesis, driving epithelial differentiation during urogenital tract development (4). PAX2 is also hypothesized to induce cell elongation and tubule formation in different types of organs, such as the inner ear, neural tube and genital tract, during embryonic development (5). In our previous study, it was demonstrated that PAX2 is crucial for maintaining epithelial cell differentiation in adult reproductive tissue (6). In the kidney, PAX2 serves an important role in the development of the collecting duct, where it induces branching morphogenesis (7,8). This was confirmed by decreased ability to form branched collecting ducts in PAX2 mutant compared with wild-type mice (8). Despite its well-established roles in normal tissue, the contribution of PAX2 to initiation and progression of ovarian cancer remains unclear. High expression levels of PAX2 in ovarian cancer cells enhance tumorigenesis in animals and are associated with shorter survival time in humans (9).

Angiogenesis is required to establish blood supply necessary for tumor growth. Anti-angiogenic therapeutic approaches have been used widely to inhibit neovascularization, but the results have been unsatisfactory in invasive and aggressive types of cancer, such as melanoma and glioblastoma (10,11). The growth of tumors, even in the presence of angiogenesis inhibiting drugs, indicates that tumor cells may have other means of promoting/obtaining blood supply (12). Anti-angiogenic therapies, such as anti-VEGF antibodies, target only endothelial cell proliferation, whereas cancerous cells may proliferate and form *de novo* vascular channels connected to endothelial-lined vasculature (13).

In 1999, Maniotis *et al* (14) observed aggressive melanoma cells forming a blood vessel-like pattern in 3D culture. When the cells were injected into mice, they formed tumors that contained vessel-like structures. This formation of vessel-like structures was termed 'vasculogenic mimicry' (VM) (14). Red

Correspondence to: Dr Kholoud Alwosaibai, Biomedical Research Department, Research Center, King Fahad Specialist Hospital, 100 Ammar Bin Thabit Street, Al Merikbat, Dammam 32253, Saudi Arabia
E-mail: kholoud.wosaibai@kfsh.med.sa

Key words: ovarian cancer, paired box 2, vascular channel, tubular channel, vasculogenic mimicry, angiogenesis, CD31, periodic acid-Schiff

blood cells are detected inside vessels, and the cells lining these vessels are negative for endothelial markers CD31 and CD34 (15). Tumor cells are organized in a pattern supported by remodeling of the extracellular matrix, as determined by periodic acid-Schiff (PAS) staining to label carbohydrates in the remodeled extracellular matrix (16).

In previous studies, CD31-negative/PAS-positive vessels formed by tumor cells demonstrated VM in *in vitro* and *in vivo* experiments (17-19). Attempts have been made to determine the molecular mechanisms underlying VM formation (20). In aggressive breast cancer cells, cyclooxygenase-2 (COX2) induces VM formation in 3D cultures and knockdown of COX2 decreases VM formation (21). Moreover, the ovarian cancer cell line SKOV3 has been reported to form VM *in vitro*; targeting CD147 in these cells causes significant downregulation of VM formation (22). CD147 is an inducer of extracellular matrix metalloproteinase (MMP)-2 (23). Overexpression of MMP has been previously linked with VM incidence in the ovarian cancer cell lines SKOV3 and OVCAR3 (24), where MMP-2 expression contributes to extracellular matrix remodeling (25). Furthermore, expression of MMP-9 has been detected in different ovarian cancer cell lines (26), and the role of MMP-9 in VM is associated with cancer progression (27).

Ovarian cancer cell lines have been reported to form VM in Matrigel culture and in xenograft mouse models (25,28). The vascular channels formed by SKOV3 and OVCAR3 ovarian cancer cells are matrix-enriched and endothelial cell-independent, and cells lining the vascular channels are positive for cytokeratin (25). Blood cells have been detected inside vascular channels formed *in vivo* (14,16). At present, the mechanism by which ovarian cancer cells promote VM is unknown. However, certain ovarian cancer cell lines express endothelial markers *de novo* and it has been hypothesized that cancer cells differentiate into endothelial cells to promote angiogenesis (13). The SKOV3 cell line has the ability to form VM in 3D culture; this may be due to weak expression of the endothelial marker CD31, which is expressed on the cell surface in monolayer cultures and in VM formed by cells (29).

Neovascularization mechanisms are key for ovarian cancer growth and dissemination to other organs (13). Our previous study found that upregulated expression of the angiogenesis biomarker CD31 may underlie the increased rate of cancer progression in a mouse model of ovarian cancer associated with high PAX2 expression (30). As these appeared to be similar to what has been previously reported for SKOV3 cells showing VM (22,29), the present study aimed to investigate the effects of PAX2 expression in epithelial cells and their ability to form branching structures when placed in 3D cultures.

Materials and methods

Human samples. Formalin-fixed paraffin-embedded (FFPE) human ovarian cancer tissue blocks were selected randomly from the cancer registry at King Fahad Specialist Hospital (Dammam, Saudi Arabia). The protocol was approved by the registered Institutional Review Board (IRB) affiliated with King Fahad Specialist Hospital-Dammam (approval no. IRB# ONC0340). The need for informed consent was waived by the IRB as the samples were archived for >10 years. Cancer tissues were assessed by independent pathologists to confirm the presence of tumor cells in the tissues before doing further experiments. The tested samples included 10 serous, four endometroid, two clear, two granulosa, one mucinous and one germ cell tumor. All 20 samples were collected from the Pathology Department and stained for PAX2 and CD31 antibodies, and PAS staining, as described in below sections, regardless of histological type. PAS staining was used to label the extracellular matrix (ECM) formed by cancer cells. The clinicopathological data including histological type, tumor status, stage and grade were collected from patient files (Table I). The age range for the 20 patients with ovarian cancer was 42-60 years old.

Cell lines. Normal mouse ovarian surface epithelial (MOSE) cells (M1102) were obtained from our previous study (9,30). Briefly, MOSE cells were isolated from the ovarian surface of 6-week-old FVB/N mice and cultured in DMEM (Thermo Fisher Scientific, Inc.) supplemented with 10% fetal bovine serum (FBS; PAA Laboratories GmbH; GE Healthcare) as described previously (30). RM ovarian cancer cells were obtained from our previous reported study (31). Briefly, RM ovarian cancer cells were derived from immortalized MOSE cells that were previously transduced with *K-Ras* ($KRAS^{G12D}$) and *c-Myc* and maintained in DMEM + 10% FBS (31).

SKOV3 human ovarian cancer cells were maintained in DMEM + 10% FBS. Immortalized HUVECs were obtained as a gift from Dr Christina Addison (Ottawa Hospital Research Institute; Ontario, Canada). HUVECs were maintained in EGM-2 media (Lonza Group, Ltd.) supplemented with 1.0 ng/ml epidermal growth factor and 10% FBS. All cell lines were incubated at 37˚C and 5% CO_2.

The M1102 and RM cells were previously modified to overexpress PAX2 (6,30) and those stably expressing cell lines were used in the present study. Briefly, lentiviral vectors were constructed by co-transfection of vector plasmids with packaging plasmid and the ecotropic envelope expression plasmid into 293T cells as described previously (32). M1102 and RM cells were infected with the lentiviral vector WPI (negative control) or lentiviral vector WPI with PAX2 gene to generate the cell lines M1102-WPI, M1102-PAX2, RM-WPI and RM-PAX2, as described previously (30). In that same study, the generation of PAX2 gene knockout cells was also described. The integrated proviruses harbor loxP sites that were excised by Cre-mediated recombination which was achieved by treating the cells with adenovirus expressing Cre recombinase (AdCre; Vector Development Laboratory) to form M1102-PAX2-AdCre cells and RM-PAX2-AdCre cells, as described previously (30).

Western blotting. The cellular proteins for M1102, M1102-WPI, M1102-PAX2 and M1102-PAX2-AdCre cells were extracted to detect PAX2 expressions using western blots as described previously (6). Briefly, cellular proteins were extracted using M-PER mammalian protein extraction reagent (Thermo Fisher Scientific, Inc.). A total of 40 μg of the extracted proteins were loaded for protein separation using 4-12% polyacrylamide gel (Thermo Fisher Scientific, Inc.), and then transferred on nitrocellulose membrane (Thermo Fisher Scientific, Inc.). The membrane was blocked using 5% non-fat milk at 4˚C for 1 h. The transferred proteins were incubated with anti-mouse PAX2 (1:20,000; cat. no. sc-130387; Santa

Table I. Clinicopathological characteristics of patients and immunohistochemical characteristics of ovarian cancer samples.

Patient sample no.	Type	Stage	Grade	Recurrent	Metastatic	Patient tumor status	CD31	PAX2	$PAS^+/CD31^-$
1	Serous	N/A	3	No	Yes	Tumor-free	High	Yes	High
2	Serous	N/A	3	No	Yes	Not tumor-free	High	No	Low
3	Serous	I	3	No	No	Not tumor-free	High	No	Low
4	Serous	IV	3	Yes	Yes	Not tumor-free	High	Yes	High
5	Serous	IV	3	Yes	Yes	Not tumor-free	Low	Yes	High
6	Serous	IV	3	Yes	yes	Not tumor-free	Low	Yes	Low
7	Serous	III	3	No	No	Tumor-free	Low	No	Low
8	Serous	IV	3	Yes	Yes	Not tumor-free	Low	No	High
9	Serous	III	3	Yes	Yes	Not tumor-free	High	No	Low
10	Serous	N/A	3	No	Yes	Not tumor-free	High	No	Low
11	Endometrioid	IV	3	Yes	Yes	Not tumor-free	Low	Yes	High
12	Endometrioid	III	3	Yes	Yes	Not tumor-free	High	No	High
13	Endometrioid	III	2	Yes	No	Tumor-free	Low	Yes	Low
14	Endometrioid	II	1	Yes	No	N/A	High	Yes	Low
15	Clear cell	IV	3	Yes	Yes	Not tumor-free	High	No	High
16	Clear cell	N/A	N/A	No	No	Tumor-free	High	Yes	High
17	Granulosa cell	III	3	Yes	Yes	Not tumor-free	High	Yes	High
18	Granulosa cell	III	N/A	Yes	Yes	Not tumor-free	High	No	High
19	Mucinous cell	IV	2	No	No	Not tumor-free	High	No	Low
20	Germ cell	III	3	Yes	Yes	N/A	High	Yes	High

PAX2, paired box 2; PAS, periodic acid-Schiff; N/A, not available.

Cruz Biotechnology, Inc.) for 1 h at room temperature, then incubated with anti-mouse horseradish peroxidase-conjugated secondary antibody (1:10,000, cat. no. 12-349; Sigma-Aldrich; Merck KGaA) for 1 h at room temperature. The immune reactivity was detected and analyzed using chemiluminescence detection kit (Clarity Western ECL Substrate; Bio-Rad Laboratories, Inc.). The protein signals were documented on the western blot membrane using FluorChem imaging system (FluorChem FC2; Alpha Innotech Corporation). The protein band densities were analyzed using ImageJ software (version 1.53a; NIH).

Animals. Animal experiments were not performed in this study. All tumor samples were obtained from tissue preserved from our previous animal experiments (9,30), which were performed in accordance with the guidelines of the Canadian Council on Animal Care and were approved by the University of Ottawa Animal Care Committee (approval no. ME-256). In that study, five female CB17 SCID mice (age, 8 weeks; weight, 17-18 g; Charles River, Montreal, Quebec) were injected in the peritoneal cavity with $1x10^7$ RM cells with or without PAX2 expression, suspended in 500 μl PBS. Animals were housed in standard rodent cages with a 12-h light/dark cycle and provided with free access to food and water. The temperature was maintained at 20-23˚C with relative humidity of 55±15%. Animals were monitored daily for disease progression and health status, noting any signs of distress or loss of wellbeing, including weight gain/loss, decreased activity, labored respiration and/or decreased ability to ambulate. Mice were euthanized when they reached a humane endpoint, such as weight gain of 15% compared with age-matched controls or abdominal distention owing to tumor and ascites formation. All animals were euthanized using CO_2 with a 50% volume displacement rate, followed by cervical dislocation. Tumor volume and total tumor mass were not assessed in the previous study (26). The solid tumor nodules were resected, fixed in 10% formalin overnight at room temperature, transferred to 70% ethanol and paraffin-embedded. The embedded tissues were retrieved from storage and used for immunohistochemistry analysis in the present study.

Matrigel (3D) culture. Eight-well chamber slides (Thermo Fisher Scientific, Inc.) were covered with 60 μl cold growth factor-reduced Matrigel (Trevigen, Inc.) and incubated at 37˚C for 30 min to polymerize the Matrigel. Each of M1102, RM, SKOV3 or HUVECs were seeded with assay medium [Mammary Epithelial Cell Growth Medium (MEGM™) supplemented with 5% FBS, 1.0 ng/ml epidermal growth factor and 0.5 ng/ml of each of insulin, hydrocortisone, cholera toxin and gentamicin]. All reagents were obtained from Lonza Group, Ltd. Different concentrations of the cells ($4x10^4$, $8x10^4$, $16x10^4$, $20x10^4$) were plated on Matrigel as described previously (33). The cells were covered with assay media containing 4% Matrigel and incubated at 37˚C for 48 h. RM cells were similarly plated; however, serum-free DMEM (Thermo Fisher Scientific, Inc.) was used in place of MEGM™. The formation of vascular channels was quantified manually by counting all

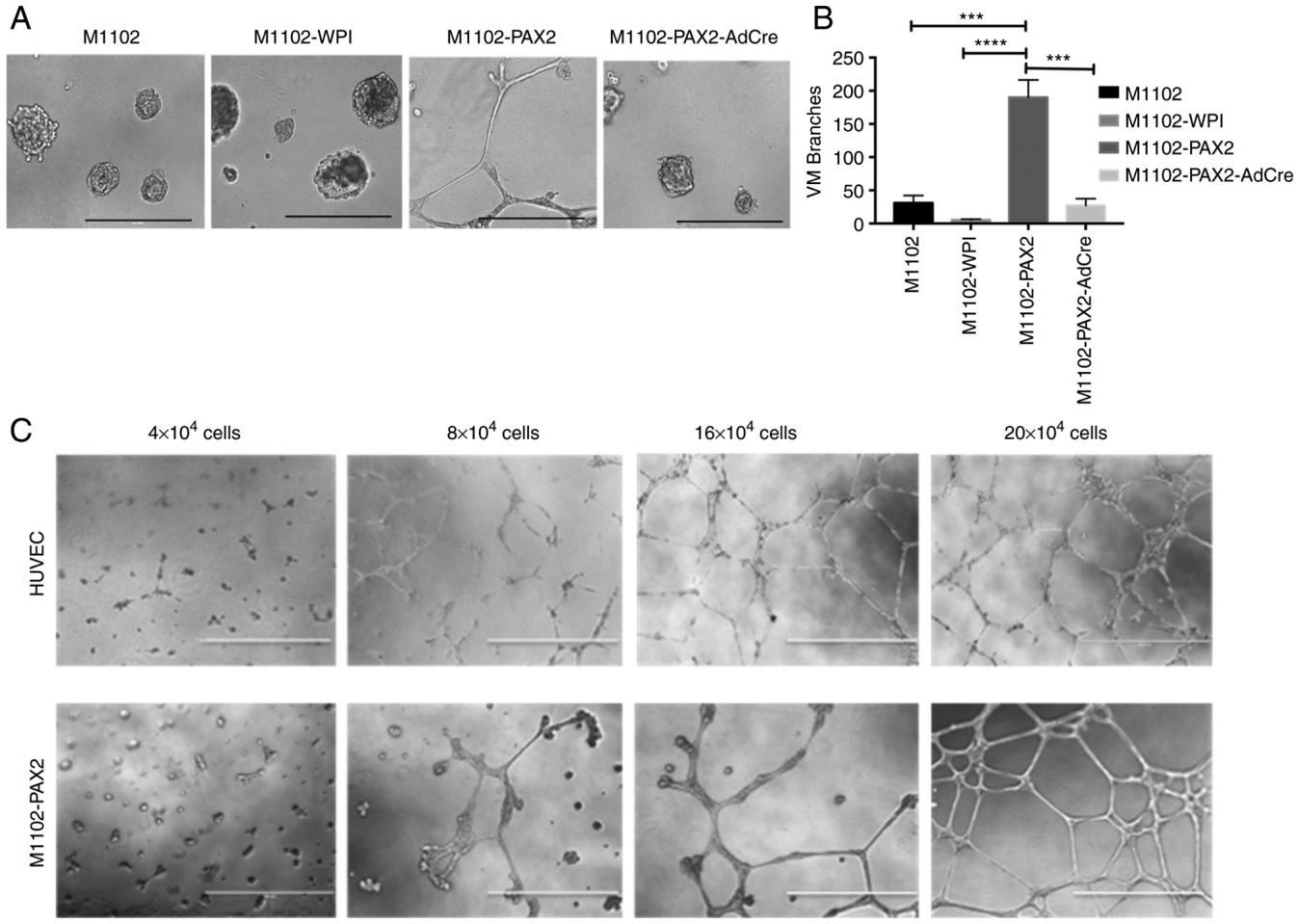

Figure 1. PAX2 induces formation of vascular-like channels in 3D culture. (A) M1102-PAX2 cells generated vascular-like channels within 48 h, whereas normal M1102 cells developed only cell aggregates. Scale bar, 400 μm. (B) Quantitative analysis of vascular-like channel branches showed a significant increase in the number of channels in M1102-PAX2 compared with parental M1102, M1102-WPI (infected with empty viral vector) and M1102-PAX2-AdCre cells (PAX2 knockout). (C) Vascular channel formation by HUVECs and M1102-PAX2 cells was associated with cell density. Scale bar, 1,000 μm. Analysis was performed using one-way ANOVA with Tukey's post hoc test. n=3; ***P<0.001 and ****P<0.0001. PAX2, paired box 2; VM, vasculogenic mimicry.

tubule branches in each well using a light microscope at 100X magnification.

Immunofluorescence analysis. Immunofluorescence analysis was performed on HUVEC, M1102-PAX2 and SKOV3 cells grown in Matrigel. The cells were fixed with 4% paraformaldehyde (Sigma-Aldrich; Merck KGaA) for 20 min and permeabilized with 1:1 methanol and acetone for 15 min, both at 4˚C. After blocking for 1 h at room temperature in 5% goat serum (Sigma-Aldrich; Merck KGaA), cells were probed with rabbit anti-CD31 (1:100; cat. no. ab222783; Abcam) for 1 h at room temperature. Alexa Fluor goat anti-rabbit IgG (1:500, cat. no. A32731; Thermo Fisher Scientific, Inc.) was used as the secondary antibody for 1 h at room temperature. The cells were mounted on Matrigel slides with VectaShield hard set mounting medium containing DAPI (Vector Laboratories, Inc.), and immunofluorescence was visualized at 100X magnification using an inverted fluorescence microscope (Axioskop 2 MOT plus) and AxioVision LE software (version 4.8.2; Carl Zeiss AG).

Immunohistochemistry. Immunohistochemistry analysis was performed on both human and animal ovarian cancer tissues. The tumor tissues were collected either from experimental animals that were injected with ovarian cancer cells or from patients that had been diagnosed with ovarian cancer, as described above. The FFPE tissues were cut into 4-μm sections, de-paraffinized and rehydrated in decreasing ethanol gradient. The tissue was heated for 10 min in a microwave in antigen unmasking solution for antigen retrieval (Vector Laboratories, Inc.). The endogenous peroxidase was neutralized in the tissues using Novocastra Peroxidase Block, 3% hydrogen peroxide (cat. no. RE7157; Leica Microsystems, Inc.). Tissue sections were blocked with Dako protein block, serum-free (Dako; Agilent Technologies, Inc.) for 1 h at room temperature. The animal tissue sections were incubated overnight at 4˚C with rabbit anti-CD31 antibody (1:100, cat. no. ab182981; Abcam) or with rabbit anti-PAX2 (1:1,000; cat. no. 71-6000; Thermo Fisher Scientific, Inc.). After washing with PBS, the animal sections were incubated with pre-diluted Dako Envision system-horseradish peroxidase (HRP) labeled polymer anti-rabbit antibodies (cat no. K4002; Dako; Agilent Technologies, Inc.) for 30 min at room temperature. The immunoreactivity was detected using DAB chromogen (50:1,000; cat. no. 8059; Cell Signaling Technology, Inc.) for 5 min at room temperature and then counterstained using hematoxylin

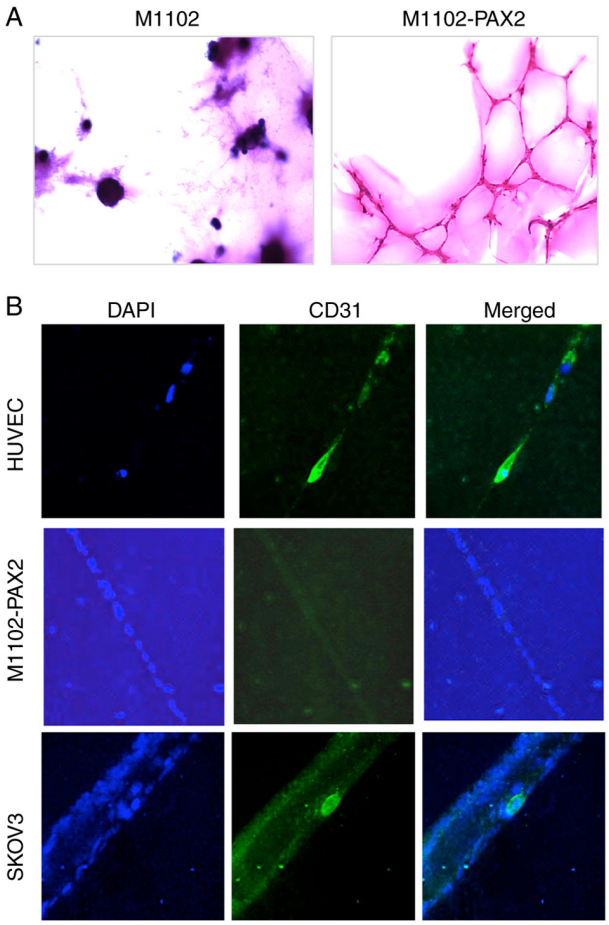

Figure 2. M1102-PAX2 cells form endothelial cell-independent vascular-like channels. (A) PAS staining for vascular-like channels formed by M1102-PAX2 cells showed pink positive staining compared with control cells not overexpressing PAX2. Magnification, 100X (B) Immunofluorescence staining for CD31 in vascular-like channels formed by HUVECs, M1102-PAX2 and SKOV3 ovarian cancer cell lines. M1102-PAX2 vascular-like channels were negative for CD31. HUVECs were used as a positive control for angiogenesis and SKOV3 cells as a positive control for VM. Few cells expressing CD31 were identified in vascular-like channels formed by SKOV3 cells. Magnification, 200X. PAS, periodic acid-Schiff; PAX2, paired box 2.

(American Master Tech Scientific, Inc.) for 1 min at room temperature. The human tissue sections were incubated for 1 h at room temperature with mouse anti-CD31 antibody (1:500; cat. no. NCL-L-CD31-607, Leica Biosystems, Inc.) or 1 h with rabbit polyclonal anti-PAX2 antibody (1:200; cat. no. 71-6000, Thermo Fisher Scientific, Inc.). After washing with PBS, human tissues were incubated with pre-diluted anti-mouse secondary antibody IgG-HRP conjugated (cat no. RE7140-CE; Leica Microsystems, Inc.) for 30 min at room temperature or goat anti-rabbit-HRP (1:500; cat. no. MP02794; Thermo Fisher Scientific, Inc.) followed by Novolink DAB chromogen (1:500; cat. no. NCL-L-CD31-60; Leica Microsystems, Inc.) for 5 min at room temperature using Novolink Polymer Detection system according to the manufacturer's instructions. The human sections were counterstained with hematoxylin for 1 min at room temperature.

Images were investigated using light microscopy, captured using the Aperio ScanScope system and analyzed using Aperio ImageScope software (version 12.3; Leica Microsystems, Inc.). Protein expression was quantified as positive pixels using the Aperio Positive Pixel Count Algorithm software (version 12.3; Leica Microsystems, Inc). The scanned tissues were carefully screened using ImageScope software to determine PAX2 expression. A minimum of 10 fields of view were investigated for PAX2 expression and four random fields were selected and images captured for analysis at 200X magnification and selected to analyze the vascular channel formation.

PAS. PAS staining was used on sections of paraffin-fixed tissues that were prepared as aforementioned or 3D cultures to stain vascular-like structures. For paraffin-fixed tissue, the fixed tissue was cut, de-paraffinized using xylene, rehydrated using graded ethanol and then heated on 95˚C for antigen retrieval using antigen unmasking solution (Vector Laboratories, Inc.). For vascular channels formed by MOSE and RM cells in 3D culture, the 8-well chamber slides were washed with PBS, fixed with 2% paraformaldehyde for 15 min at room temperature and then washed with PBS three times. PAS staining was performed using PAS kit (Sigma-Aldrich; Merck KGaA) according to the manufacturer's protocol for both FFPE sections and 3D culture. Periodic acid (250 μl/well or section) was added at room temperature for 5 min, and then washed with PBS 3-5 times for 5 min each. Schiff stain (250 μl/well or section) was added at room temperature for 15 min and washed three times for 5 min each. All washing was performed using PBS (500 μl/well or section). All washing steps for the wells were performed using a pipette to drop the solution on top of the Matrigel. For the double staining of PAS and antibody in FFPE tissues, PAS staining was performed following DAB and hematoxylin staining for the immunohistochemistry analysis.

Evaluation of the staining. All stained and scanned human tissues were analyzed using light microscopy (magnification, 200X). The positive index was applied to evaluate PAX2, CD31 and PAS staining. For PAX2, ≥30% of positively nuclear staining out of the total stained tissue was considered as PAX2-positive. For evaluating the stained vessels, the staining evaluation was performed based on assessing all stained vessels in all inspected fields in the tissues. If >50% of the vessels of the inspected fields were stained with CD31 and/or PAS, the evaluations were considered as $CD31^{high}$ and/or PAS^{high}; while <50% were considered as $CD31^{low}$ and/or PAS^{low}. The evaluation of VM after the dual staining of CD31 and PAS was observed in each field by detecting vessels that were $CD31^{-}/PAS^{+}$. Detecting >30% of the vessels that were $CD31^{-}/PAS^{+}$ was considered as VM-positive tissues and <30% was considered as negative.

Statistical analysis. All experiments were performed at least three times. Image analysis was performed using Aperio Positive Pixel Count Algorithm (version 12.3; Leica Microsystems, Inc.) and ImageJ (National Institutes of Health). The quantification of PAX2, CD31 and PAS expression levels were determined based on positive pixel counts relative to tissue area. Statistical analysis was performed using GraphPad Prism (versions 7 and 9; GraphPad Software, Inc.). An unpaired Student's t-test (for two groups) or one way ANOVA with post hoc Tukey's test (for >2 groups) was used to determine statistical significance. Data are presented as the

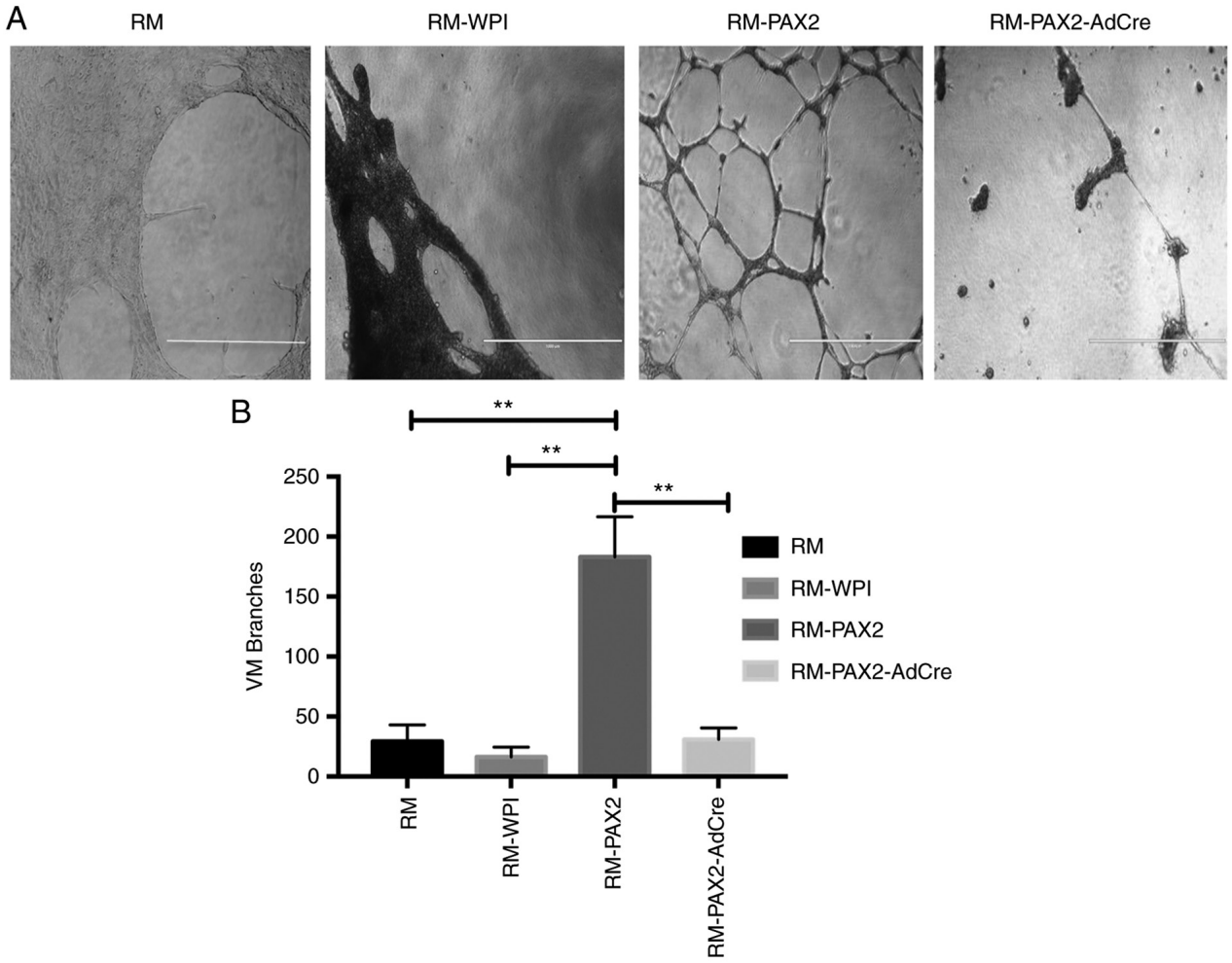

Figure 3. PAX2 induces formation of vascular-like channels in RM mouse ovarian cancer cells in 3D culture. (A) RM-PAX2 cells differentiated in Matrigel to form vascular-like channels, whereas RM and RM-WPI control cells did not form organized web-like tubular channels. Scale bar, 1,000 μm. (B) Quantitative analysis of the total number of vascular channel branches formed by RM-PAX2 cells showed they were significantly more abundant compared with the parental RM, RM-WPI (transfected with empty viral vector) and RM-PAX2-AdCre (PAX2 knockout) cells. Data were compared using one-way ANOVA with Tukey's post hoc test. n=3; **P<0.01. PAX2, paired box 2; VM, vasculogenic mimicry.

mean ± standard error of the mean. P<0.05 was considered to indicate a statistically significant difference.

Results

PAX2 induces vascular-like channels in MOSE cells in vitro. The overexpression and knockout of PAX2 in M1102 cells was confirmed using western blotting (Fig. S1), as reported in our previous study (6). To determine whether PAX2 induces formation of vascular-like channels by normal epithelial cells, M1102-PAX2 cells were plated in 3D cultures using Matrigel. M1102-PAX2 cells exhibited branching and elongation to form vascular-like channels that mimicked vascular channels formed by endothelial cells (Fig. 1). By contrast, parental and vector control M1102 cells did not form vascular-like channels, and knockout of Pax2 by AdCre decreased formation of vascular-like channels relative to their PAX2-expressing counterparts (Fig. 1A). The statistical analysis of tubule formation showed a significant increase in the number of tubular branches formed by M1102-PAX2 compared with M1102, M1102-WPI or M1102-PAX2-AdCre (Fig. 1B). Formation of vascular-like channels was associated with cell density, in which the higher the number of plated cells, the more organized the branched vascular channels were after 48 h (Fig. 1C and Data S1); HUVECs were used as a positive control.

PAX2 induces endothelial cell-independent vascular-like channels. To determine whether PAX2 induced the differentiation of epithelial to endothelial cells and the formation of vascular-like channels, the formed channels were stained with PAS to label ECM formed by M1102-PAX2 cells. The glycogen in the ECM reacts with PAS, which stains tissue dark purple. Oxidized glycogens (aldehydes) are detected by the PAS stain, which results in a pink color in the tissue (34). The vascular-like channels formed by M1102-PAX2 cells were PAS-positive, which indicated the presence of ECM supporting vascular-like channels, whereas spheres formed by control M1102 cells were PAS-negative (Fig. 2A). Furthermore, vascular-like channels formed by M1102-PAX2 cells were CD31-negative, unlike HUVEC cells, suggesting that PAX2 did not induce ovarian epithelial differentiation to endothelial cells but did induce formation of vascular-like channels. HUVEC cells were used as a positive control for endothelial cells expressing CD31. SKOV3 cells were included as a positive control for

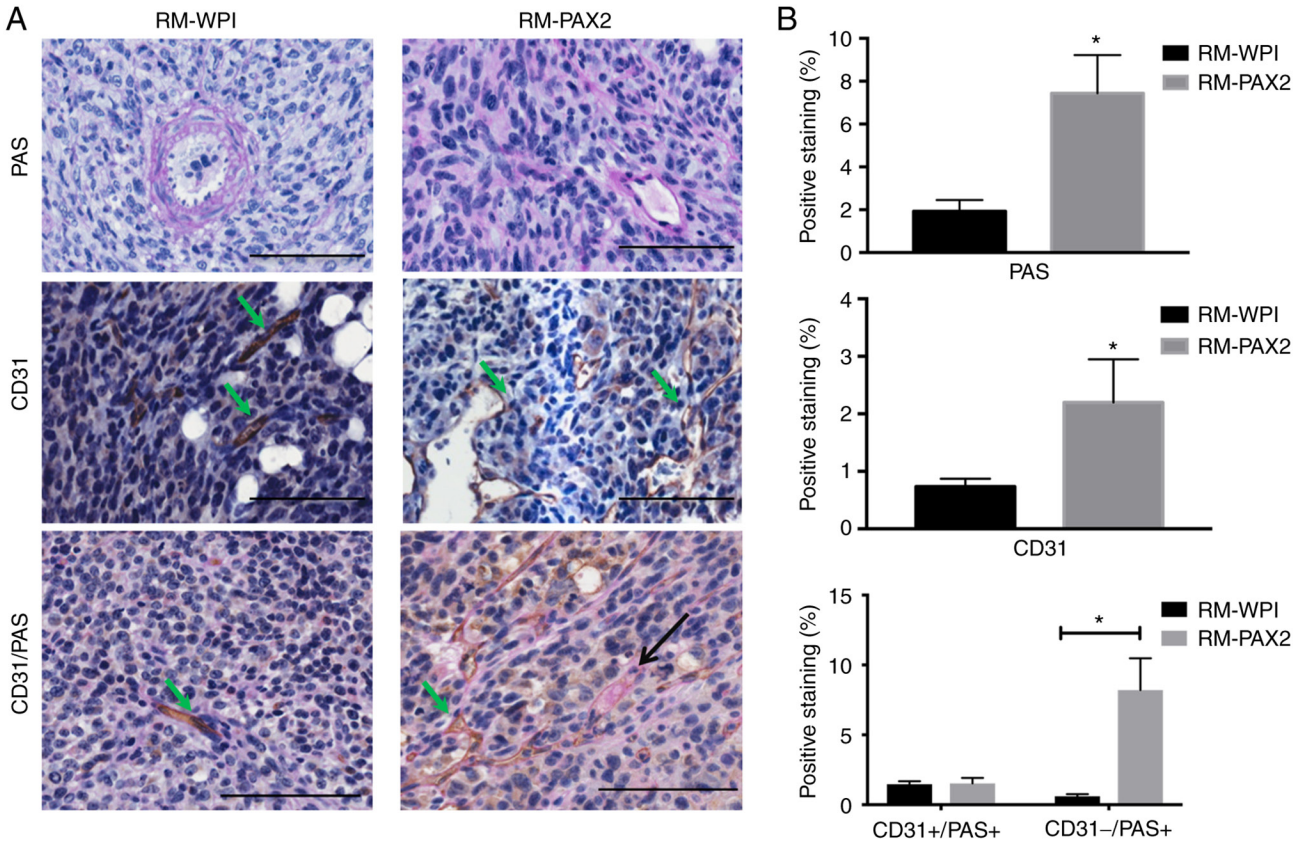

Figure 4. PAS and CD31 immunohistochemical staining of tumors formed in mice by RM-WPI and RM-PAX2 cell xenografts. (A) Tumors derived from RM-WPI (transfected with empty viral vector) and RM-PAX2 cells showed vascular-like channels positive for PAS staining (upper panels). CD31 staining in vascular channels in a RM-PAX2 tumor indicated that PAX2 enhanced angiogenesis [green arrows indicate the existence of regular vessels (angiogenesis); middle panels]. Double staining for CD31 and PAS (lower panels). $PAS^+/CD31^+$ vascular-channels were present in both RM-WPI and RM-PAX2 tumors (green arrows). $CD31^-/PAS^+$ lumen may have been indicative of vasculogenic mimicry in RM-PAX2 tumors (black arrow). Scale bar, 100 μm. (B) Quantification of CD31 and PAS immunohistochemical staining. Analysis was performed by measuring the percentage of positive pixels in three different areas from RM-WPI and RM-PAX2 cancers. Image analysis was performed using Aperio Positive Pixel Count Algorithm software. Statistical analysis was performed using unpaired Student's t-test. $^*P<0.05$ vs. RM-WPI. PAS, periodic acid-Schiff; PAX2, paired box 2.

assessment of vascular channel formation, as it has been previously reported that they do not express CD31 normally (25) but form vascular channels in 3D culture (22). SKOV3 cells readily formed vascular-like channels and cells within those channels differentiated and expressed CD31 (Fig. 2B).

PAX2 enhances vascular-like channel formation in RM ovarian cancer cells in vitro. To determine whether PAX2 enhanced vascular channel formation by cancer cells, tumors derived from the RM mouse ovarian cancer cell line was used. To determine whether RM cells that overexpressed PAX2 induced vascular-like channel formation, the ability of these cells to elongate and form branched channels in Matrigel was assessed. Overexpression of PAX2 in RM cells significantly enhanced formation of vascular-like channels in Matrigel compared with RM and RM-WPI control cells, which did not form vascular-like channels in Matrigel. Moreover, RM-PAX2-AdCre cells that had PAX2 knocked out exhibited significantly decreased formation of vascular-like channels compared with RM-PAX2 (Fig. 3A and B).

PAX2 enhances vascular-like channel formation in tumors formed by RM cells in vivo. To determine the role of PAX2 in inducing tumor progression in a model of ovarian cancer, RM-WPI or RM-PAX2 cells were injected into immunocompromised mice. Both RM-WPI and RM-PAX2 cells developed tumors in injected mice. RM-PAX2 tumors exhibited small vascular-like channels that were PAS-positive, whereas RM-WPI tumors lacked small vascular-like channels and PAS staining labeled large blood vessels (Fig. 4A). RM-PAX2 tumors also exhibited a higher density of CD31-stained vessels compared with RM-WPI tumors (Fig. 4A), suggesting that PAX2 enhanced angiogenesis in these ovarian cancer cells. To determine if RM-PAX2 tumors induced *de novo* vessel formation, PAS/CD31 double staining was performed. RM-PAX2 tumors possessed both types of vascular channels; those formed by endothelial cells that were PAS- and CD31-positive, whereas small vascular channels that were not formed by endothelial cells were PAS-positive but CD31-negative (Fig. 4A and B). Since VM is PAS-positive/CD31-negative (12), these results suggested that PAX2 may have enhanced tumor progression by inducing vasculogenesis.

To confirm whether cancer cells expressing PAX2 formed vascular-like channels, tumors derived from RM-WPI and RM-PAX2 cells were stained for PAX2, PAS and CD31. Tumors arising from RM-PAX2 cells exhibited vascular channels lined with cells expressing PAX2 and contained

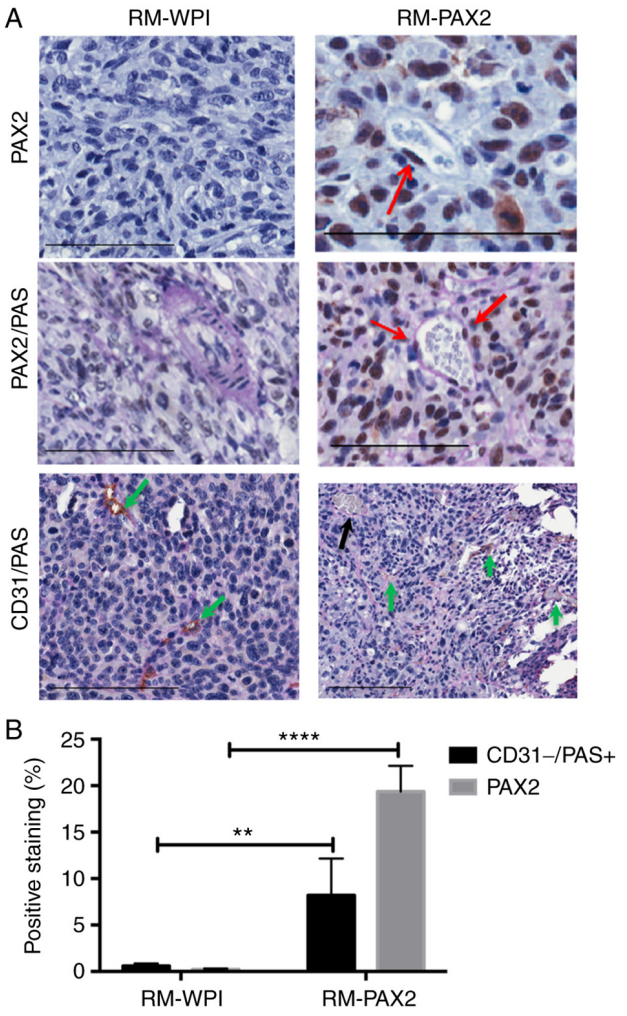

Figure 5. PAX2 is expressed in the cells lining vascular-like channels and is associated with VM. (A) PAX2 is expressed in the nucleus of RM-PAX2 tumors (red arrows), whereas RM-WPI (transfected with empty vector) tissue was PAX2-negative (upper panels). RM-WPI possessed PAS-positive (pink) vascular channels only in large vessels (middle panels). In RM-PAX2 tumors, vessels were stained with PAS, with some cells lining channels positive for PAX2 (red arrows). The lower panels show the double staining for CD31 and PAS on PAX2-negative tumor sections (RM-WPI) and PAX2-positive tumor sections (RM-PAX2). RM-WPI showed $CD31^+/PAS^+$ staining, indicating regular blood vessels (green arrows). In RM-PAX2 tumors, $CD31^+/PAS^+$ staining indicated blood vessels (green arrows) and $CD31^-/PAS^+$ staining indicated VM formation (black arrow). Scale bar, 100 μm. (B) Quantification of immunohistochemical detection of PAX2 and $CD31^-/PAS^+$ showed an increase in PAX2 and $CD31^-/PAS^+$ staining in RM-PAX2 compared with RM-WPI tumors, indicating that expression of PAX2 was associated with increased VM. Image analysis was performed using Aperio Positive Pixel Count Algorithm software. Analysis was performed using unpaired Student's t-test for three different fields of the tumor section. **P<0.01, ****P<0.0001. PAS, periodic acid-Schiff; PAX2, paired box 2; VM, vasculogenic mimicry.

red blood cells (Fig. 5A). Double staining showed vessels lined with PAX2-expressing cells stained positive for PAS and contained red blood cells, indicative of a blood vessel. The sections that exhibited PAX2 expression contained both CD31-positive/PAS-positive vessels, indicating regular blood vessels and CD31-negative/PAS-positive vessels, suggesting vasculogenesis in these tumors (Fig. 5A and B). However, RM-WPI tumors were negative for PAX2, as expected and exhibited CD31-positive/PAS-positive vessels, indicating regular blood vessels that were formed by endothelial cells. These observations indicated that PAX2 contributed to formation of vascular channels in ovarian tumors.

PAX2 is associated with tubular-like structures in human ovarian cancer. To investigate whether PAX2 expression was associated with specific histological and tissue structures, the histological subtypes of human ovarian cancer tissue were investigated. PAX2 immunohistochemical staining showed the presence of cells that expressed nuclear PAX2 in certain ovarian cancer samples (Figs. 6 and S2).

A total of four (40%) serous carcinoma tissue samples expressed nuclear PAX2 (Table II). However, three samples that expressed PAX2 showed high PAS staining and low CD31 expressions, indicative of vasculogenic activity in these tissues. The serous carcinoma samples that showed high vasculogenic activity were not associated with specific ovarian cancer grade or stage. Furthermore, three cases (75%) of endometrioid carcinoma expressed PAX2. However, only one sample showed high PAX2 expression, high PAS staining and low CD31 expression. Only one sample of each of the other ovarian cancer histological types (clear, granulosa and germ cell tumors) exhibited vasculogenic activity.

Serous ovarian carcinoma cells expressing PAX2 exhibited different morphological structures compared with endometrioid ovarian cancer. Serous ovarian carcinoma that expressed PAX2 showed tubular- or papillary-like structures (Fig. 6), whereas in endometrioid ovarian cancer tissue, PAX2 expression was associated with solid and unbranched masses that possessed CD31-negative blood vessels (Fig. S2). Moreover, serous tumor cells that exhibited high levels of PAX2 were associated with low levels of CD31, indicating a decreased number of blood vessels (Fig. 6). CD31/PAS staining showed similar results. CD31 expression was notably lower compared with PAS staining in PAX2-positive human tumor tissue (Fig. 6). By contrast, PAX2-negative tumor tissue was associated with high levels of CD31 expression in endothelial cells that lined the blood vessels (Fig. S3). This indicated that PAX2-negative tissues exhibited increased levels of angiogenesis and lacked vasculogenesis (Fig. S3). Unlike animal tumors that were generated using RM-PAX2 cancer cells and presented high angiogenesis activity, human ovarian tumors had decreased angiogenesis by endothelial cells in PAX2-positive tissues and induced *de novo* vascular formation.

Discussion

The role of PAX2 in ovarian cancer is poorly understood; however, previous studies suggested that expression of PAX2 alone does not induce OSE cell transformation into cancerous cells (9,30). However, the ability of PAX2 to promote vascular-like channels suggests that tumors that express PAX2 may be more aggressive owing to the development of vascular-like channels that augment tumor blood supply in the absence of angiogenesis (35).

Normal OSE cells do not express PAX2 (30), whereas 61% of ovarian cancer cell lines express PAX2 (3), suggesting a potential oncogenic role for PAX2 in cancer derived from ovarian epithelium. The oncogenic role of PAX2 in ovarian cancer has been investigated in terms of its ability to promote cell proliferation, migration and tumor formation (9,30). The

Table II. Number of ovarian cancer samples stained positive for PAX2, PAS and CD31, to show the vasculogenic activity of each histological type of ovarian cancer.

Histological type	Total, n	$PAX2^{+}$, n (%)	$PAX2^{+}/PAS^{high}$, n	PAX^{+}/PAS^{low}, n	$PAX2^{-}/PAS^{high}$, n	$CD31^{low}$, n
Serous carcinoma	10	4 (40)	3	0	1	3
Endometroid carcinoma	4	3 (75)	1	2	1	2
Clear cell	2	1 (50)	1	1	0	0
Granulosa cell	2	1 (50)	1	0	1	0
Mucinous cell	1	0 (0)	0	0	0	0
Germ cell tumor	1	1 (100)	1	0	0	0

PAX2, paired box 2; PAS, periodic acid-Schiff.

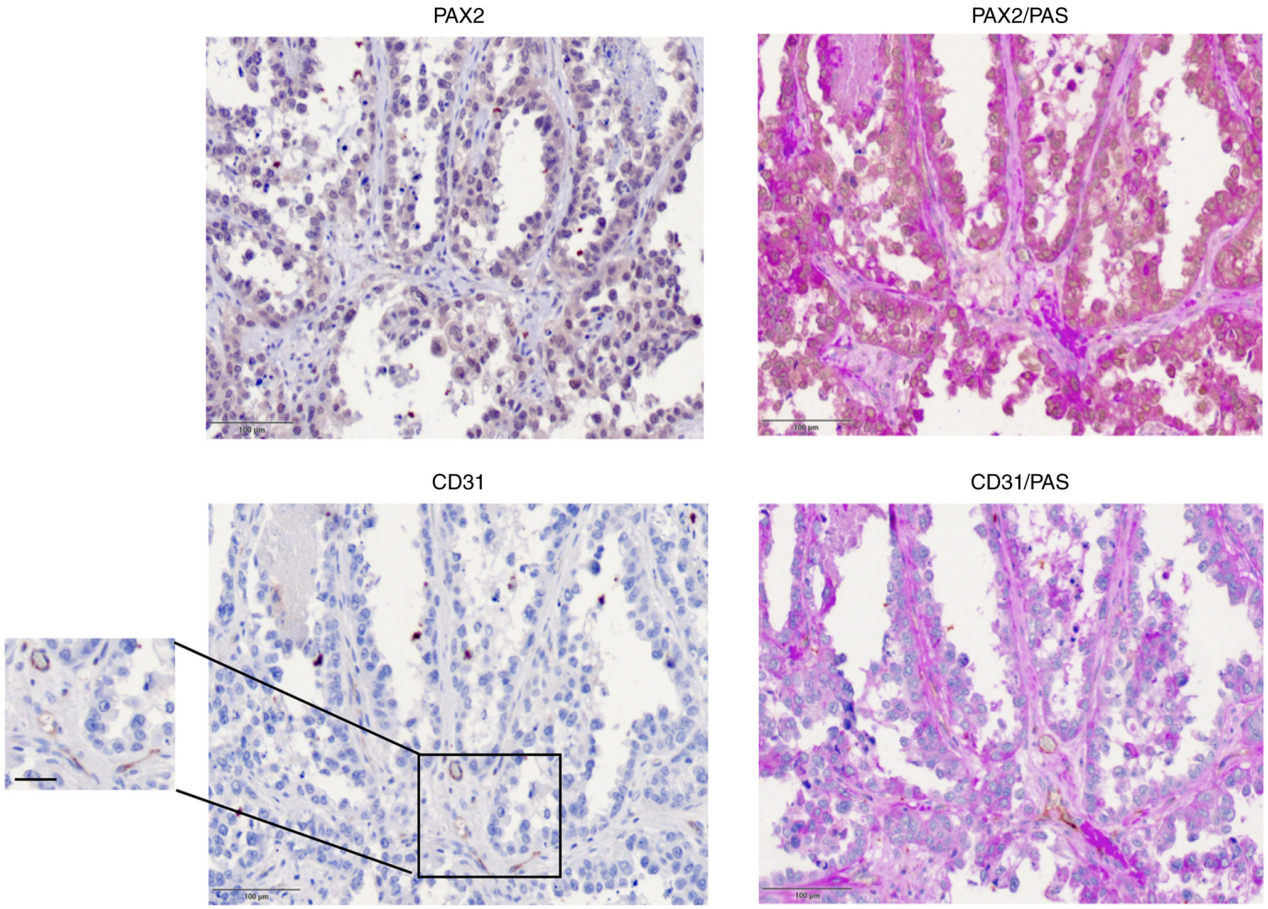

Figure 6. PAX2 immunohistochemical staining of human serous ovarian cancer. Human ovarian tumor sections showed tubule-like structures lined with cells that expressed PAX2 and basement membrane stained positive for PAS. Few CD31-positive vessels were observed. Scale bar, 100 μm (original) and 20 μm (magnified). PAS, periodic acid-Schiff; PAX2, paired box 2.

present investigation of the ability of PAX2 to promote epithelial differentiation of MOSE cells revealed that PAX2 expression in M1102 MOSE cells induced formation of vascular-like structures in Matrigel, whereas the control groups did not form these structures. The ability to form vessel-like structures is associated with aggressive tumor cells, such as those present in melanoma (14), and is known as VM. Unlike MOSE cells, normal expression of PAX2 in mouse oviductal epithelial cells does not allow for VM, but enhances the formation of hollow lumen structures under the same 3D culture conditions (6), resembling acini-like structures that are formed by normal mammary epithelial cells (33).

HUVEC endothelial cells commonly form vascular networks in 3D culture, and this type of cellular organization has been used as a standard measure of the potential for cellular vasculogenesis (36). However, to the best of our knowledge, no other normal cells have been reported to possess this capability. Aggressive cancer cells such as melanoma form *de novo* webs of vessels (14). In the present study, vascular-like channels formed by M1102-PAX2 in Matrigel were morphologically

similar to vessels formed by HUVECs and VM networks formed by SKOV3 ovarian cancer cells, providing the first evidence of such capacity in normal non-endothelial cells.

Vascular-like channels in M1102-PAX2 cells were supported by remodeling of the ECM, which was positive for PAS and negative for CD31. However, SKOV3 VM resulted in few cells expressing CD31, which is consistent with a previous report suggesting that cancer cells may differentiate into endothelial cells *de novo* to induce angiogenesis (29). Thus, it was hypothesized that PAX2 could induce vascular-like channels *in vitro* in normal MOSE cells. Vascular-like channel induction in M1102 cells by PAX2 was not the result of stem cell differentiation, as our previous study showed that PAX2 decreases stemness in MOSE cells (6). However, it was not possible to investigate vessel formation *in vivo* with normal MOSE-PAX2 cells since these cells do not form tumors when injected into mice (30).

RM mouse ovarian cancer cells are tumorigenic in mice and overexpression of PAX2 results in increased rate of tumor progression (30). To investigate the potential role of PAX2 in VM during tumor progression, the present study investigated RM cells *in vitro* and *in vivo*. It was revealed that overexpression of PAX2 in RM cells significantly increased formation of vascular-like channels *in vitro*. In addition, RM-PAX2 was revealed to increase both VM and angiogenesis *in vivo*, as determined by staining the cancer tissues for CD31 and PAS. Some of the neo-vasculature was determined to be CD31-negative and PAS-positive, indicating that PAX2 induces cancer cells to form VM. Certain cells lining those vessels expressed PAX2 in the nucleus, suggesting that cancer cells that express PAX2 may contribute to formation of neo-vasculature in the tumor.

The molecular mechanism by which PAX2 promotes vascular channels has not yet been established, although it may be mediated by COX2 expression. As PAX2 induces COX2 in RM cells (30) and COX2 induces VM in breast cancer (21), it is hypothesized that PAX2-induced VM may be mediated by COX2 expression. Moreover, PAX2 may also regulate vascular channels through MMP activity; the role of MMPs during morphogenesis, tissue remodeling and VM has been widely reported (37,38). In ovarian cancer, overexpression of MMPs is associated with ECM remodeling (25), cancer progression (26,27) and poor prognosis (39). Previous studies support the role of MMPs in the formation of tubular-like structures and VM in cancer cell lines (39,40). However, targeting the MMP-2 inducer CD147 in SKOV3 cells resulted in significantly decreased formation of CD31-negative/PAS-positive vessels (22). Whether PAX2 regulates MMP expression in ovarian cancer cells, and whether this contributes to the underlying mechanism involved in induction of vascular channels, remains to be determined.

PAX2 has been reported to induce tubular branching in the kidney and elongation of inner ear precursors (41), as well as serving a role in fallopian tube morphogenesis (30), which may occur via a similar mechanism to VM in ovarian cancer cells. To the best of our knowledge, few studies have reported expression levels of PAX2 in ovarian cancer. One study showed that PAX2 is upregulated in papillary serous ovarian cancer (42). Another study showed a higher percentage of low-grade serous cancer exhibits increased PAX2 expression compared with high-grade cancer (43). PAX2-positive cells have been detected in non-serous ovarian cancer, including endometrioid (33%), mucinous (17%) and clear cell carcinoma (35% of cases) (3). In the present study, PAX2 was associated with the web-like structures in certain subtypes of ovarian cancer such as serous and endometrioid carcinoma. The tumor subtypes that exhibited high PAX2 and low CD31 expression were associated with decreased angiogenesis. However, PAX2 expression was associated with increased PAS staining, which was indicative of the level of VM. These findings indicated that PAX2 may induce formation of tubular structures or vascular-like channels in serous cancer that is not associated with a high degree of angiogenesis. However, PAX2 expression is associated with poorer prognosis in patients with serous ovarian cancer (9). The p53 status is also significantly associated with patient survival. Wild-type p53 is associated with a significant decrease in progression-free survival rate (44), which may indicate that ovarian tumors that have high PAX2 expression and wild-type P53 exhibit a high degree of VM associated with more aggressive tumors.

To the best of our knowledge, the potential role of PAX2 in the formation of vascular-like channels in ovarian cancer is a novel finding. In the present study, overexpression of PAX2 promoted formation of tubular-like channels both *in vitro* and *in vivo*. In established ovarian tumors, PAX2 may enhance tumor progression and metastasis by VM, which allows increased blood supply to the tumor. In a similar fashion, high expression levels of PAX2 in renal tumor-derived endothelial cells are associated with angiogenesis and VM that enhance tumor growth (35). However, the role of PAX2 in cancer cells may be context dependent. Previous studies have demonstrated the oncogenic role of PAX2 in ovarian, prostate and melanoma cancer cells (9,30,45-47), whereas other studies found that PAX2 exerts a tumor suppressive role in different types of ovarian cancers (48,49). Thus, the role of PAX2 in enhancing vascular-like structures may depend on the specific cancer type and genetic profile of cancer cells.

The present study had certain limitations. The M1102 normal epithelial cells and RM cancer ovarian cell line were derived from mice. Human ovarian cancer cell lines derived from specific histological subtypes of ovarian cancer should be used to determine the capacity for vasculogenesis and involvement of PAX2 in each subtype. In addition, antibody staining of cells grown in Matrigel was limited owing to the difficulties in performing this experiment. However, staining vascular channels with other antibodies including vascular endothelial cadherin, vascular endothelial growth factor receptor and MMPs should be performed in future to further characterize VM (50). Cancer tissue that exhibited vasculogenesis expressed PAX2 in the nucleus. However, it was not possible to directly assess whether PAX2 induced vasculogenic activity in human ovarian cancer tissues and whether tubular-like channels were formed by PAX2-positive cells. Although multiple vascular-like structures that contained blood cells were found, whether PAX2 induced cell elongation to form web-like structures or vessel formation to supply blood remains to be confirmed. Investigating PAX2 expression in different types of human ovarian cancer cells using confocal and electron microscopy should also be performed to determine if tubular structures are lined with cells expressing PAX2 and form hollow structures that contain blood cells in

3D culture and cancer tissue. In addition, molecular signaling that mediates vasculogenesis in different types of ovarian cancer cells was not assessed. The role of PAX2 downstream signaling and genes involved in mediating PAX2 function in tubular structure formation remain to be determined.

Acknowledgements

Not applicable.

Funding

The present study was supported by Canadian Institutes of Health Research and King Fahad Specialist Hospital-Dammam.

Availability of data and materials

The datasets used and/or analyzed during the current study are available from the corresponding author on reasonable request.

Authors' contributions

KA and EMA made substantial contributions to the conception and design of the current study. EMA and SA performed the experiments and collected data. BCV, KG and SG made significant contributions to data analysis and interpretation. BCV and KG revised the manuscript for important intellectual content. KA and BCV confirmed the authenticity of all the raw data. All authors read and approved the final manuscript.

Ethics approval and consent to participate

The protocols related to the animal experiments were approved by the University of Ottawa Animal Care Committee (approval no. ME-256). The protocols related to human tissues were approved by the ethical committee that affiliated with King Fahad Specialist Hospital-Dammam (approval no. IRB# ONC0340). The informed consents for the patients were waived by IRB.

Patient consent for publication

Not applicable.

Competing interests

The authors declare that they have no competing interests.

References

1. Krzystyniak J, Ceppi L, Dizon DS and Birrer MJ: Epithelial ovarian cancer: The molecular genetics of epithelial ovarian cancer. Ann Oncol 27 (Suppl 1): i4-i10, 2016.
2. Bogdanova N and Dörk T: Molecular genetics of breast and ovarian cancer: Recent advances and clinical implications. Balkan J Med Genet 15 (Suppl): S75-S80, 2012.
3. Song H, Kwan SY, Izaguirre DI, Zu Z, Tsang YT, Tung CS, King ER, Mok SC, Gershenson DM and Wong KK: PAX2 expression in ovarian cancer. Int J Mol Sci 14: 6090-6105, 2013.
4. Eccles MR, He S, Legge M, Kumar R, Fox J, Zhou C, French M and Tsai RW: PAX genes in development and disease: The role of PAX2 in urogenital tract development. Int J Dev Biol 46: 535-544, 2002.
5. Terzić J, Muller C, Gajović S and Saraga-Babić M: Expression of PAX2 gene during human development. Int J Dev Biol 42: 701-707, 1998.
6. Alwosaibai K, Abedini A, Al-Hujaily EM, Tang Y, Garson K, Collins O and Vanderhyden BC: PAX2 maintains the differentiation of mouse oviductal epithelium and inhibits the transition to a stem cell-like state. Oncotarget 8: 76881-76897, 2017.
7. Narlis M, Grote D, Gaitan Y, Boualia SK and Bouchard M: Pax2 and pax8 regulate branching morphogenesis and nephron differentiation in the developing kidney. J Am Soc Nephrol 18: 1121-1129, 2007.
8. Mansouri A, Hallonet M and Gruss P: Pax genes and their roles in cell differentiation and development. Curr Opin Cell Biol 8: 851-857, 1996.
9. Feng Y, Tang Y, Mao Y, Liu Y, Yao D, Yang L, Garson K, Vanderhyden BC and Wang Q: PAX2 promotes epithelial ovarian cancer progression involving fatty acid metabolic reprogramming. Int J Oncol 56: 697-708, 2020.
10. Piao Y, Liang J, Holmes L, Henry V, Sulman E and de Groot JF: Acquired resistance to anti-VEGF therapy in glioblastoma is associated with a mesenchymal transition. Clin Cancer Res 19: 4392-4403, 2013.
11. Helfrich I, Scheffrahn I, Bartling S, Weis J, von Felbert V, Middleton M, Kato M, Ergün S, Augustin HG and Schadendorf D: Resistance to antiangiogenic therapy is directed by vascular phenotype, vessel stabilization, and maturation in malignant melanoma. J Exp Med 207: 491-503, 2010.
12. Folberg R, Hendrix MJ and Maniotis AJ: Vasculogenic mimicry and tumor angiogenesis. Am J Pathol 156: 361-381, 2000.
13. Tang HS, Feng YJ and Yao LQ: Angiogenesis, vasculogenesis, and vasculogenic mimicry in ovarian cancer. Int J Gynecol Cancer 19: 605-610, 2009.
14. Maniotis AJ, Folberg R, Hess A, Seftor EA, Gardner LM, Pe'er J, Trent JM, Meltzer PS and Hendrix MJ: Vascular channel formation by human melanoma cells in vivo and in vitro: vasculogenic mimicry. Am J Pathol 155: 739-752, 1999.
15. Racordon D, Valdivia A, Mingo G, Erices R, Aravena R, Santoro F, Bravo ML, Ramirez C, Gonzalez P, Sandoval A, *et al*: Structural and functional identification of vasculogenic mimicry in vitro. Sci Rep 7: 6985, 2017.
16. Valdivia A, Mingo G, Aldana V, Pinto MP, Ramirez M, Retamal C, Gonzalez A, Nualart F, Corvalan AH and Owen GI: Fact or fiction, it is time for a verdict on vasculogenic mimicry? Front Oncol 9: 680, 2019.
17. Itzhaki O, Greenberg E, Shalmon B, Kubi A, Treves AJ, Shapira-Frommer R, Avivi C, Ortenberg R, Ben-Ami E, Schachter J, *et al*: Nicotinamide inhibits vasculogenic mimicry, an alternative vascularization pathway observed in highly aggressive melanoma. PLoS One 8: e57160, 2013.
18. Dong X, Sun B, Zhao X, Liu Z, Gu Q, Zhang D, Zhao N, Wang J and Chi J: Expression of relative-protein of hypoxia-inducible factor-1α in vasculogenesis of mouse embryo. J Biol Res (Thessalon) 21: 4, 2014.
19. Luo F, Yang K, Liu RL, Meng C, Dang RF and Xu Y: Formation of vasculogenic mimicry in bone metastasis of prostate cancer: Correlation with cell apoptosis and senescence regulation pathways. Pathol Res Pract 210: 291-295, 2014.
20. Qiao L, Liang N, Zhang J, Xie J, Liu F, Xu D, Yu X and Tian Y: Advanced research on vasculogenic mimicry in cancer. J Cell Mol Med 19: 315-326, 2015.
21. Basu GD, Liang WS, Stephan DA, Wegener LT, Conley CR, Pockaj BA and Mukherjee P: A novel role for cyclooxygenase-2 in regulating vascular channel formation by human breast cancer cells. Breast Cancer Res 8: R69, 2006.
22. Millimaggi D, Mari M, D'Ascenzo S, Giusti I, Pavan A and Dolo V: Vasculogenic mimicry of human ovarian cancer cells: Role of CD147. Int J Oncol 35: 1423-1428, 2009.
23. Sun J and Hemler ME: Regulation of MMP-1 and MMP-2 production through CD147/extracellular matrix metalloproteinase inducer interactions. Cancer Res 61: 2276-2281, 2001.
24. Sood AK, Fletcher MS, Coffin JE, Yang M, Seftor EA, Gruman LM, Gershenson DM and Hendrix MJ: Functional role of matrix metalloproteinases in ovarian tumor cell plasticity. Am J Obstet Gynecol 190: 899-909, 2004.
25. Sood AK, Seftor EA, Fletcher MS, Gardner LM, Heidger PM, Buller RE, Seftor RE and Hendrix MJ: Molecular determinants of ovarian cancer plasticity. Am J Pathol 158: 1279-1288, 2001.

26. Labrie M, Vladoiu MC, Grosset AA, Gaboury L and St-Pierre Y: Expression and functions of galectin-7 in ovarian cancer. Oncotarget 5: 7705-7721, 2014.
27. Lin H, Pan JC, Zhang FM, Huang B, Chen X, Zhuang JT, Wang H, Mo CQ, Wang DH and Qiu SP: Matrix metalloproteinase-9 is required for vasculogenic mimicry by clear cell renal carcinoma cells. Urol Oncol 33: 168.e9-e16, 2015.
28. Ayala-Domínguez L, Olmedo-Nieva L, Muñoz-Bello JO, Contreras-Paredes A, Manzo-Merino J, Martínez-Ramírez I and Lizano M: Mechanisms of vasculogenic mimicry in ovarian cancer. Front Oncol 9: 998, 2019.
29. Su M, Feng YJ, Yao LQ, Cheng MJ, Xu CJ, Huang Y, Zhao YQ and Jiang H: Plasticity of ovarian cancer cell SKOV3ip and vasculogenic mimicry in vivo. Int J Gynecol Cancer 18: 476-486, 2008.
30. Al-Hujaily EM, Tang Y, Yao DS, Carmona E, Garson K and Vanderhyden BC: Divergent roles of PAX2 in the etiology and progression of ovarian cancer. Cancer Prev Res (Phila) 8: 1163-1173, 2015.
31. Yao DS, Li L, Garson K and Vanderhyden BC: The mouse ovarian surface epithelium cells (MOSE) transformation induced by c-myc/K-ras in. Zhonghua Zhong Liu Za Zhi 28: 881-885, 2006 (In Chinese).
32. Kutner RH, Zhang XY and Reiser J: Production, concentration and titration of pseudotyped HIV-1-based lentiviral vectors. Nat Protoc 4: 495-505, 2009.
33. Debnath J, Muthuswamy SK and Brugge JS: Morphogenesis and oncogenesis of MCF-10A mammary epithelial acini grown in three-dimensional basement membrane cultures. Methods 30: 256-268, 2003.
34. Vigier S and Fülöp T: Exploring the extracellular matrix to create biomaterials. In: Composition and Function of the Extracellular Matrix in the Human Body [Internet]. Travascio F (ed). IntechOpen, Rijeka, 2016. https://doi.org/10.5772/62979.
35. Fonsato V, Buttiglieri S, Deregibus MC, Puntorieri V, Bussolati B and Camussi G: Expression of Pax2 in human renal tumor-derived endothelial cells sustains apoptosis resistance and angiogenesis. Am J Pathol 168: 706-713, 2006.
36. Ponce ML: Tube formation: An in vitro matrigel angiogenesis assay. Methods Mol Biol 467: 183-188, 2009.
37. Sivak JM, Mohan R, Rinehart WB, Xu PX, Maas RL and Fini ME: Pax-6 expression and activity are induced in the reepithelializing cornea and control activity of the transcriptional promoter for matrix metalloproteinase gelatinase B. Dev Biol 222: 41-54, 2000.
38. Marchenko GN, Marchenko ND and Strongin AY: The structure and regulation of the human and mouse matrix metalloproteinase-21 gene and protein. Biochem J 372: 503-515, 2003.
39. Mariya T, Hirohashi Y, Torigoe T, Tabuchi Y, Asano T, Saijo H, Kuroda T, Yasuda K, Mizuuchi M, Saito T and Sato N: Matrix metalloproteinase-10 regulates stemness of ovarian cancer stem-like cells by activation of canonical Wnt signaling and can be a target of chemotherapy-resistant ovarian cancer. Oncotarget 7: 26806-26822, 2016.
40. Rodriguez JA, Orbe J, De Lizarrondo SM, Calvayrac O, Rodriguez C, Martinez-Gonzalez J and Paramo JA: Metalloproteinases and atherothrombosis: MMP-10 mediates vascular remodeling promoted by inflammatory stimuli. Front Biosci 13: 2916-2921, 2008.
41. Christophorou NAD, Mende M, Lleras-Forero L, Grocott T and Streit A: Pax2 coordinates epithelial morphogenesis and cell fate in the inner ear. Dev Biol 345: 180-190, 2010.
42. Tong GX, Chiriboga L, Hamele-Bena D and Borczuk AC: Expression of PAX2 in papillary serous carcinoma of the ovary: Immunohistochemical evidence of fallopian tube or secondary Müllerian system origin? Mod Pathol 20: 856-863, 2007.
43. Tung CS, Mok SC, Tsang YT, Zu Z, Song H, Liu J, Deavers MT, Malpica A, Wolf JK, Lu KH, *et al*: PAX2 expression in low malignant potential ovarian tumors and low-grade ovarian serous carcinomas. Mod Pathol 22: 1243-1250, 2009.
44. Wong KK, Izaguirre DI, Kwan SY, King ER, Deavers MT, Sood AK, Mok SC and Gershenson DM: Poor survival with wild-type TP53 ovarian cancer? Gynecol Oncol 130: 565-569, 2013.
45. Ueda T, Ito S, Shiraishi T, Kulkarni P, Ueno A, Nakagawa H, Kimura Y, Hongo F, Kamoi K, Kawauchi A and Miki T: Hyper-expression of PAX2 in human metastatic prostate tumors and its role as a cancer promoter in an in vitro invasion model. Prostate 73: 1403-1412, 2013.
46. Lee SB, Doberstein K, Baumgarten P, Wieland A, Ungerer C, Bürger C, Hardt K, Boehncke WH, Pfeilschifter J, Mihic-Probst D, *et al*: PAX2 regulates ADAM10 expression and mediates anchorage-independent cell growth of melanoma cells. PLoS One 6: e22312, 2011.
47. Hardy LR, Salvi A and Burdette JE: UnPAXing the divergent roles of PAX2 and PAX8 in high-grade serous ovarian cancer. Cancers (Basel) 10: 262, 2018.
48. Raffone A, Travaglino A, Saccone G, Mascolo M, Insabato L, Mollo A, De Placido G and Zullo F: PAX2 in endometrial carcinogenesis and in differential diagnosis of endometrial hyperplasia: A systematic review and meta-analysis of diagnostic accuracy. Acta Obstet Gynecol Scand 98: 287-299, 2019.
49. Gruss P and Walther C: Pax in development. Cell 69: 719-722, 1992.
50. Luo Q, Wang J, Zhao W, Peng Z, Liu X, Li B, Zhang H, Shan B, Zhang C and Duan C: Vasculogenic mimicry in carcinogenesis and clinical applications. J Hematol Oncol 13: 1-15, 2020.